

Spatial spread of the Hantavirus infection

José A. Reinoso* and F. Javier de la Rubia†

*Departamento de Física Fundamental, Universidad Nacional de Educación a Distancia-UNED,
Paseo Senda del Rey 9, E-28040 Madrid, Spain*

(Received 28 July 2014; revised manuscript received 10 February 2015; published 9 March 2015)

The spatial propagation of Hantavirus-infected mice is considered a serious threat for public health. We analyze the spatial spread of the infected mice by including diffusion in the stage-dependent model for Hantavirus infection recently proposed by Reinoso and de la Rubia [*Phys. Rev. E* **87**, 042706 (2013)]. We consider a general scenario in which mice propagate in fronts from their refugia to the surroundings and find an expression for the speed of the front of infected mice. We also introduce a depletion time that measures the time scale for an appreciable impoverishment of the environment conditions and show how this new situation may change the spreading of the infection significantly.

DOI: [10.1103/PhysRevE.91.032703](https://doi.org/10.1103/PhysRevE.91.032703)

PACS number(s): 87.19.xd, 87.23.Cc, 05.45.—a

I. INTRODUCTION

In 1993 the deer mouse, *Peromyscus maniculatus*, the most widespread mammal in the United States, was identified as the host of a new kind of Hantavirus [1,2], named sin nombre virus (SNV), which causes a severe disease in humans called pulmonary Hantavirus syndrome (HPS), a disease with a mortality rate as high as 40%. Despite the large number of studies made since then, no successful vaccine has been obtained [3]. In order to understand the appearance and propagation of the disease, and eventually prevent its effects, different attempts have been carried out to understand the major features that characterize the population dynamics of deer mice.

In this way, several simplified models have been introduced that come to describe many of the known characteristics of the process in the long term [4–6]. The models consider the same well-known basic processes (birth, death, competition, and transmission of the infection through contact mainly among adults) and have as a fundamental parameter the carrying capacity, K , whose variations are very sensitive to climatic changes. These climatic variations play a fundamental role in the evolution of the population of mice, which is directly related with the appearance and propagation of the infection [7,8]. All the models present a transcritical bifurcation controlled by a critical carrying capacity, K_c , that characterizes the dynamics. Above it, the system evolves to a state with infected mice, and below the critical value, the infection does not occur. However, there are significant differences among them, and in Ref. [6] we considered a division of the population in terms of age and incorporated the effect of the initial infection-free period (due, for instance, to the transfer of maternal antibodies) and the maturation time to become an adult mouse susceptible to be infected [9,10].

An important aspect of the spreading of the infection is the spatial propagation of mice from refugia to its surroundings. This has already been analyzed in the original AK model and some of its variants [4,5,11,12].

In this work we study the spatial spreading of the infection in the model introduced in Ref. [6]. We set a scenario where waves of mice propagate and characterize its main features such as stationarity, speed of fronts, and infection. In Sec. I, we introduce and describe the model. Sections II and III are devoted to the numerical and analytical study of the model in a general scenario. We particularize the scenario in Sec. IV to consider a depletion time of the landscape resources. Finally, in Sec. V we present some concluding remarks.

II. MODEL

One fundamental characteristic of the Hantavirus infection is that the mice are born free from the infection, and this condition is maintained for an appreciable period of time. To include this fact in the analysis of the propagation of the Hantavirus, in Ref. [6] we proposed a homogeneous stage-dependent model with three variables: M_Y , M_{As} , and M_{Ai} , representing the density of virus-free young mice, adults susceptible to being infected by the virus, and adults already infected, respectively. The model evolves in agreement with the following processes: births, deaths, competition for the resources, transmission of the infection among adults, and maturation of the young mice to become susceptible adults (mice that were born in $t - \tau$ and were able to survive until a time t become adults susceptible to contracting the virus). With all these ingredients, the model is

$$\frac{dM_Y}{dt} = bM - cM_Y - \frac{M_Y M}{K} - be^{-\gamma\tau} M(t - \tau), \quad (1)$$

$$\frac{dM_{As}}{dt} = be^{-\gamma\tau} M(t - \tau) - cM_{As} - \frac{M_{As} M}{K} - aM_{As} M_{Ai}, \quad (2)$$

$$\frac{dM_{Ai}}{dt} = -cM_{Ai} - \frac{M_{Ai} M}{K} + aM_{As} M_{Ai}, \quad (3)$$

where $M = M_Y + M_{Ai} + M_{As}$ and a , b , c , K , γ , and τ are positive parameters. The different terms on the right-hand sides of Eqs. (1)–(3) represent the following processes: births with rate b , deaths for natural reasons with rate c , competition for the resources characterized by the carrying capacity K , transmission of the virus with rate a , and maturation of the

*aparicioreinoso@gmail.com

†jrubia@fisfun.uned.es

young mice with a time constant τ and depletion risk parameter γ describing the difficulty of passing from youth to adulthood. We refer the reader to Ref. [6] for the details and features of the model.

To go a step further one has to consider that the deer mouse changes eventually its burrow, particularly after leaving its dam, looking for a new one in its surroundings [11]. To describe this process, we generalize the homogeneous model (1)–(3) by introducing diffusive terms to characterize the movement of the mice population on a two-dimensional space. However, this diffusive movement also affects the maturation process, since a mouse born in $t - \tau$ at point (x, y) , and that remains alive, becomes an adult at point (x_0, y_0) . Therefore, assuming the mice are performing an unbiased random walk, we have to consider the diffusion process over the distance between the birth and maturation points, and following Ref. [13] we replace each one of the two delayed terms appearing in the homogeneous model by the term

$$\frac{be^{-\gamma\tau}}{4\pi D_Y\tau} \int_{-\infty}^{\infty} \int_{-\infty}^{\infty} e^{-[(x-x_0)^2+(y-y_0)^2]/4D_Y\tau} M(x, y, t-\tau) dx dy, \quad (4)$$

where D_Y is the diffusion coefficient for the young mice population, and the integration takes into account the contributions from the whole domain.

Moreover, in this space-dependent model the carrying capacity will depend now on time and space $K(x_0, y_0, t)$. This change is substantial since the dynamics is characterized by the critical value $K_c = be^{\gamma\tau}/[a(b-c)]$ that marks the onset of the infection and therefore defines a map of refugia, in which the infection prevails. If the circumstances change, as we describe in the next sections, there will be a diffusive movement from refugia to uninfected areas, that differs for young and adults, and controlled by the diffusion coefficients D_Y and D_A , respectively.

With all these ingredients, we study the propagation of infection on a two-dimensional space. To make things simpler, we also consider the model with axial symmetry and use polar coordinates (r, θ) . With this simplifying assumption the diffusion operator is $\frac{\partial^2}{\partial x^2} + \frac{\partial^2}{\partial y^2} = \frac{\partial^2}{\partial r^2} + \frac{1}{r} \frac{\partial}{\partial r}$ and we can integrate the angular variable in the maturation term to make it depend only on the radial variable

$$\begin{aligned} & \frac{be^{-\gamma\tau}}{4\pi D_Y\tau} \int_0^{\infty} \rho M(\rho, t-\tau) d\rho \int_{-\pi}^{\pi} e^{-(r^2+\rho^2-2\rho r \sin\theta)/4D_Y\tau} d\theta \\ &= \frac{be^{-\gamma\tau}}{2D_Y\tau} \int_0^{\infty} e^{-(r^2+\rho^2)/4D_Y\tau} I_0(r\rho/2D_Y\tau) \rho M(\rho, t-\tau) d\rho \end{aligned} \quad (5)$$

with $I_0(r\rho/2D_Y\tau)$ as the modified Bessel function of the first kind [14].

In this situation, the model takes advantage of the axial symmetry and depends only on the distance, r . It reads

$$\begin{aligned} \frac{\partial M_Y}{\partial t} &= D_Y \left(\frac{\partial^2 M_Y}{\partial r^2} + \frac{1}{r} \frac{\partial M_Y}{\partial r} \right) + bM - cM_Y - \frac{M_Y M}{K(r, t)} \\ &- \frac{be^{-\gamma\tau}}{2D_Y\tau} \int_0^{\infty} e^{-(r^2+\rho^2)/4D_Y\tau} I_0(r\rho/2D_Y\tau) \\ &\times \rho M(\rho, t-\tau) d\rho, \end{aligned} \quad (6)$$

$$\begin{aligned} \frac{\partial M_{As}}{\partial t} &= D_A \left(\frac{\partial^2 M_{As}}{\partial r^2} + \frac{1}{r} \frac{\partial M_{As}}{\partial r} \right) - cM_{As} - \frac{M_{As} M}{K(r, t)} \\ &- aM_{As} M_{Ai} + \frac{be^{-\gamma\tau}}{2D_Y\tau} \int_0^{\infty} e^{-(r^2+\rho^2)/4D_Y\tau} \\ &\times I_0(r\rho/2D_Y\tau) \rho M(\rho, t-\tau) d\rho, \end{aligned} \quad (7)$$

$$\begin{aligned} \frac{\partial M_{Ai}}{\partial t} &= D_A \left(\frac{\partial^2 M_{Ai}}{\partial r^2} + \frac{1}{r} \frac{\partial M_{Ai}}{\partial r} \right) - cM_{Ai} - \frac{M_{Ai} M}{K(r, t)} \\ &+ aM_{As} M_{Ai}. \end{aligned} \quad (8)$$

Note that if we add Eqs. (6)–(8) we obtain an equation governing the evolution of the total number of mice, $M = M_Y + M_{As} + M_{Ai}$,

$$\begin{aligned} \frac{\partial M}{\partial t} &= D_Y \left(\frac{\partial^2 M_Y}{\partial r^2} + \frac{1}{r} \frac{\partial M_Y}{\partial r} \right) + D_A \left(\frac{\partial^2 M_A}{\partial r^2} + \frac{1}{r} \frac{\partial M_A}{\partial r} \right) \\ &+ (b-c)M - \frac{M^2}{K(r, t)}, \end{aligned} \quad (9)$$

where $M_A = M_{As} + M_{Ai}$. When $D_Y = D_A = D$, Eq. (9) is the well-known Fisher's equation, extensively studied in the literature [15,16].

In general terms, we may expect the system (6)–(8) having wavelike solutions moving with an r -dependent velocity. However, for large-enough r the $1/r$ terms in the equations become negligible, and the wavelike solutions end up being traveling wave fronts moving with a constant velocity [16]. The numerical analysis of the system shows that this is indeed the case and that after a short transient and for moderate values of r the system spreads within well-defined fronts.

III. SCENARIO

The infection under harsh environmental conditions survives only in a limited number of places called refugia in which $K_1 > K_c$ (we denote by K_1 the generic carrying capacity of the refugia). However, some changes in the environment may be significant enough to trigger a migration movement from the refugia, with the mice invading the surrounding landscape looking for an ecological opportunity. Where this ecological opportunity is high, the corresponding carrying capacity, K_2 , is also high. If $K_2 > K_c$ the infection could appear in that area, while for $K_2 < K_c$ no infection arises.

In the following we analyze numerically and analytically the scenario with $K_1 > K_c$ and $K_2 > K_c$ and discuss the main features of the propagation. We consider as initial conditions a finite number of mice, some of them infected, in the refugia and no mice in the surroundings.

A. Numerical studies

To study numerically the model (6)–(8) we take the following values for the parameters: $a = 0.4$, $b = 2$, $c = 0.6$, $D_Y = 5 D_A = 2.5$, $\tau = 2$, and $\gamma = 0.7$ leaving K as variable [4,6,11].

An example of the spatial spreading of mice at a given time and the temporal evolution at a given point is depicted in Figs. 1 and 2.

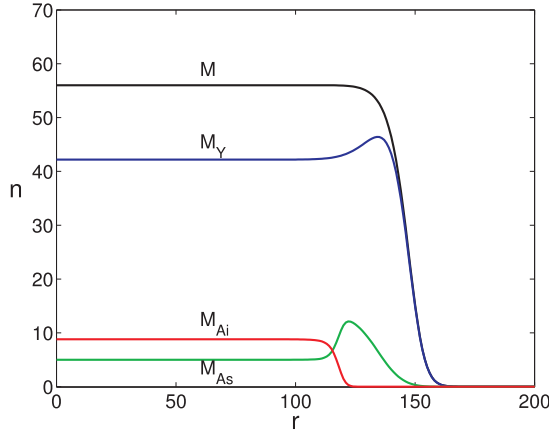


FIG. 1. (Color online) Spatial distribution of the spreading of mice from a refugium at a time $t = 19$ for $K_1 = K_2 = 40 > K_c = 14.48$. The curve labeled M represents the total number of mice. Other system parameters are indicated in the main text.

Mice spread from the refugium, located in the middle of the domain. After a transient, when r is large enough, the spreading enters a state where mice move out within well-defined fronts. First, healthy mice, mainly young mice, M_Y , and new susceptible adults, M_{As} , invade the domain at a constant speed (independent of K_2) and at a rate given by a logistic growth. This defines the M front, the vanguard of mice. Later, the wave of infection arises, propagating asymptotically to a constant speed, lower or equal to the speed of the M front, depending on the value of K . This general behavior is depicted in Fig. 3.

B. Analytical results

We consider the set of fronts that move from the refugium to its surroundings. After the transient we may neglect the $1/r$ terms in Eqs. (6)–(9), and each front starts moving at a constant speed (see Fig. 3). If we then shift the frame of reference to the comoving frame, fronts look frozen, and we can get rid of

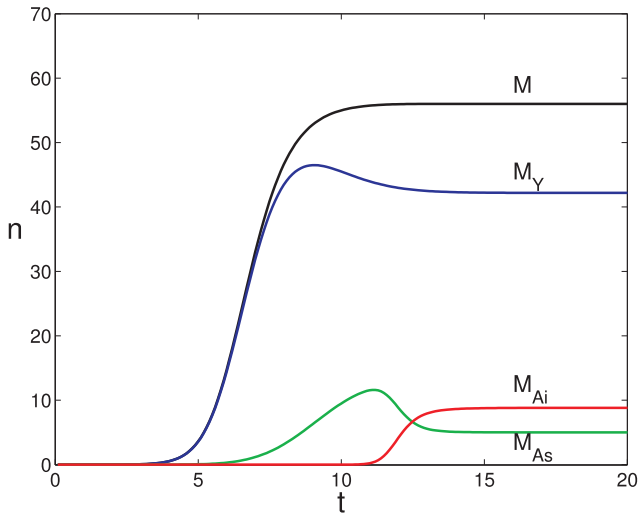


FIG. 2. (Color online) Temporal evolution of the mice spreading at the point $x = 78$. Parameters as in Fig. 1.

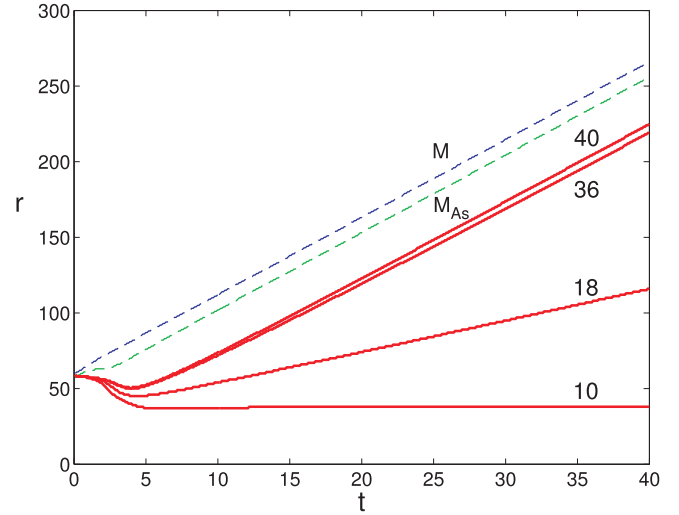


FIG. 3. (Color online) Propagation of fronts in time. The two dashed lines depict the M and M_{As} fronts, respectively, propagating at the same speed. The solid lines represent M_{Ai} fronts for different values of K . For $K = 40$ and $K = 36$, the speeds go asymptotically to the same speed as the M and M_{As} fronts, while for $K = 18$ the speed is lower. The curve for $K = 10$ represents a front that does not move, as in this case $K < K_c = 14.48$.

the temporal dependence in Eqs. (6)–(8) and (9). Since at the leading edge of the propagating front M is the sum of M_Y and M_{As} , it is enough to consider the fronts of M and M_{Ai} . We have

$$(b-c)M - \frac{M^2}{K(r,t)} + D_Y \frac{d^2 M_Y}{dr^2} + D_A \frac{d^2 M_A}{dr^2} + v_M \frac{dM}{dr} = 0, \quad (10)$$

$$-cM_{Ai} - \frac{M_{Ai}M}{K(r,t)} + aM_{As}M_{Ai} + D_A \frac{d^2 M_{Ai}}{dr^2} + v_{M_{Ai}} \frac{dM_{Ai}}{dr} = 0. \quad (11)$$

The way to analyze these equations to obtain the speed of the fronts is standard [16]. We approach each front as an abrupt transition between two homogeneous solutions. For the M front, we study it locally at the border with the no mice solution and write $M = \delta M$, $M_Y = \delta M_Y$, $M_{As} = \delta M_{As}$, $M_{Ai} = \delta M_{Ai}$. Moreover, at that point the front is mainly made of young mice and the wave of adults has not arrived yet (see Fig. 1). It is, therefore, justified to assume $d\delta M_A/dr \approx 0$ and $\delta M_Y \approx \delta M$. Substituting in (10) and retaining only first-order terms, we get

$$v_M \frac{d\delta M}{dr} + D_Y \frac{d^2 \delta M}{dr^2} + (b-c)\delta M = 0. \quad (12)$$

If we now analyze its eigenvalues, considering that the front is not oscillatory, we obtain a criteria for the speed of the front, and the minimum speed (which is the one observed in the numerical simulations [11]) is

$$v_M = 2\sqrt{D_Y(b-c)}. \quad (13)$$

The front of infected mice (M_{Ai} front) is studied in the same way, performing a linear stability analysis around the

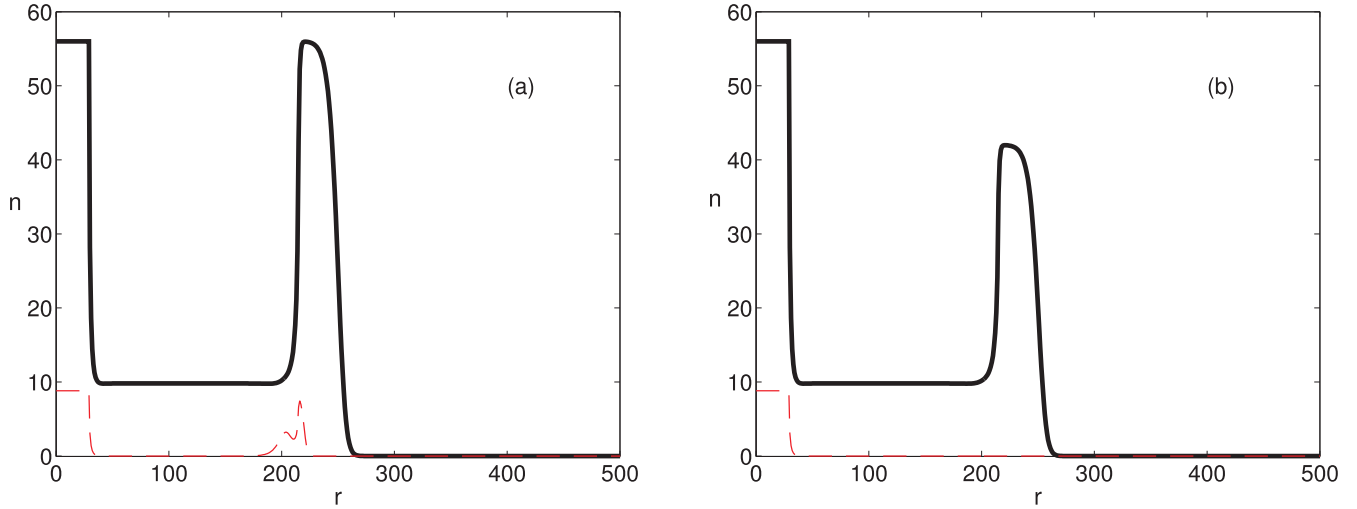


FIG. 4. (Color online) Spatial distribution of mice for an scenario with depletion time (solid line: M front; dashed line: M_{Ai} front). After a time τ_d , the original carrying capacity of the region, K_2 , diminishes to a new value, K_3 . (a) $K_1 = K_2 = 40 > K_0$, $K_3 = 7$. (b) $K_1 = 40$, $K_2 = 30 < K_0$, $K_3 = 7$. The infection propagates in (a) but it does not in (b). System parameters as in Fig. 1 ($K_c = 14.48$, $K_o = 34.76$).

homogeneous unstable stationary state, $M = K(b - c)$, $M_Y = K(b - c)(1 - e^{-\gamma\tau})$, $M_{As} = K(b - c)e^{-\gamma\tau}$, $M_{Ai} = 0$, leading to

$$v_{M_{Ai}} \frac{d\delta M_{Ai}}{dr} + D_A \frac{d^2\delta M_{Ai}}{dr^2} + [ae^{-\gamma\tau}K(b - c) - b]\delta M_{Ai} = 0 \quad (14)$$

and performing an analysis of the eigenvalues under the same conditions as before of a nonoscillatory front, we obtain the minimum speed

$$v_{M_{Ai}} = 2\sqrt{D_A[aK(b - c)e^{-\gamma\tau} - b]}. \quad (15)$$

It is interesting to notice the effect of the risk parameter (γ) or the maturation time (τ) in the above equation. As compared with the AK model [11], both parameters lower the propagation speed of the infection.

From (13) and (15) we see that $v_{M_{Ai}} \leq v_M$ for $K \leq K_0$, where

$$K_0 = \frac{[D_Y(b - c) + D_{AB}]e^{\gamma\tau}}{a(b - c)D_A} > K_c. \quad (16)$$

The numerical simulation of the model confirms this behavior for $K_c < K < K_0$ and, moreover, shows that when $K_0 < K$ all fronts move at a common speed given by the speed of the M front (see Fig. 3).

IV. SCENARIO WITH DEPLETION TIME

In many cases, the ecological opportunity, which implies a high carrying capacity, is limited in time by resource depletion. This may happen by the proper action of the mice in the region or by the effect of external changes due to climatic or human causes. It is therefore reasonable to consider a

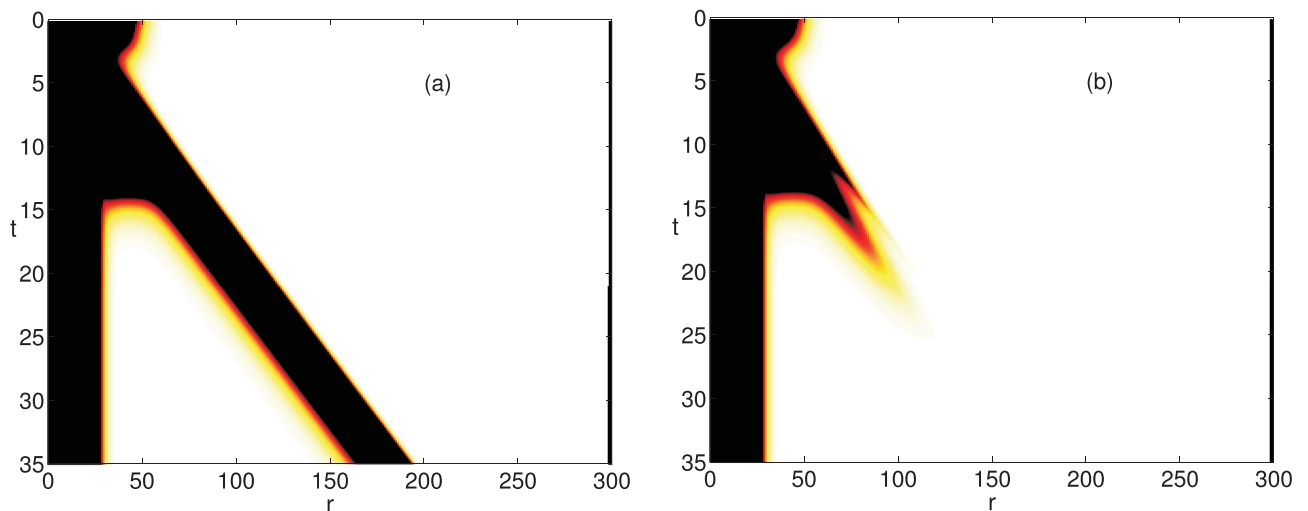


FIG. 5. (Color online) Same scenarios as in Fig. 4, depicted in space and time. (a) The infection propagates at a constant speed as a soliton-like solution. (b) The structure is dissipative and the infection disappears after a short time.

depletion time, τ_d , to measure the time scale for an appreciable change in the environment conditions. When this happens, the corresponding carrying capacity in the region decreases from K_2 to a new value, K_3 . When $K_3 < K_c$ there may be a significant change in the propagation of the infection depending on the previous value K_2 . When $K_2 > K_0$, then $v_{M_{Ai}} = v_M$ and the infection propagates in space as a soliton-like solution, but if $K_c < K_2 < K_0$ ($v_{M_{Ai}} < v_M$), this solution is dissipative and the infection stops propagating after a short time. These two possibilities are depicted in Figs. 4 and 5.

As a first approximation to measure the dissipation time of the propagated infection, we consider constant speeds. The initial length traveled by the front of infection before the drastic decrease of K due to the depletion is given by $\Delta x = v_{M_{Ai}}(\tau_d - \tau_i)$, where τ_i is the time interval between the front of mice and the front of infected ones at the beginning. For the propagation of infected mice τ_i must be lower than τ_d . The expression for the dissipation time is

$$\tau_d = \frac{v_{M_{Ai}}}{(v_M - v_{M_{Ai}})}(\tau_d - \tau_i). \quad (17)$$

V. CONCLUDING REMARKS

The spatial propagation of the Hantavirus infection is a concern for human communities close to mice reservoirs. In this work we have extended the model proposed in Ref. [6] to consider spatial diffusion and axial symmetry. In this scenario the mice spread out from their refugia, where they overcome harsh conditions, to their surroundings following several waves. Young and susceptible adults are at the leading edge, while the infection, which also spreads from the refugia and is carried by infected mice, comes at a later time. A complementary approach between analytical and numerical studies shows that, after a transient, fronts evolve at stationary speeds. When $K > K_0 > K_c$ both fronts have equal speeds, while if $K_c < K < K_0$ the front of infection, which is behind the vanguard of mice, lags at a constant speed. Moreover, the risk parameter and the maturation time, which are distinctive

ingredients of our model, may play an important role in establishing the speed of the infection wave.

By introducing a depletion time in the surroundings, we have shown that the scenario may change significantly. In particular, depending on the values of the carrying capacity of the region the infection may propagate as a soliton-like solution or may become dissipative and vanish after a short time. For the soliton-like solution, at a given point in the surroundings, the infection arrives as a wave and lasts a finite time before the infection disappears.

As a result of our analysis, three theoretical ways to control the infection spreading have emerged:

(1) $K_2 < K_c$. The carrying capacity in the surroundings of the refugium is maintained lower than the critical value, so the infection cannot be propagated in space. This is the most basic way to control the infection.

(2) $K_2 > K_c$ and $\tau_i > \tau_d$. Even if the carrying capacity is over the critical value, we could control the depletion time. If it is shorter than the time it takes the infection to get there, τ_i , there will be no propagation of the infection.

(3) $K_2 > K_c$, $\tau_i < \tau_d$, and $K_2 < K_0$. As a last possibility to control the spread of the infection, its speed has to be lower than the M -front speed, and in this case the infection does not propagate too long.

Finally, we would like to note that in many regions of South America, the spreading of mice from their refugia (“ratada” in Spanish) has been widely observed during the past few centuries [17]. In particular, the Colilargo mouse (*Oligoryzomys longicaudatus*), which is the main host of the Andes virus, a Hantavirus that can be transmitted among humans, has been involved in the 2011 ratada in western Argentina [18].

ACKNOWLEDGMENTS

This work has been financially supported by the Ministerio de Ciencia e Innovación (Spain), Project No. FIS2009-09870. J.A.R. also acknowledges support from Grant No. BES-2008-003398.

-
- [1] S. Nichol, C. Spiropoulou, S. Morzunov, P. Rollin, T. Ksiazek, H. Feldmann, A. Sanchez, J. Childs, S. Zaki, and C. Peters, *Science* **262**, 914 (1993).
- [2] J. E. Childs, G. Ksiazek, C. F. Spiropoulou, J. W. Krebs, and S. Morzunov, *J. Infect. Dis.* **169**, 1271 (1994).
- [3] C. B. Jonsson, J. Hooper, and G. Mertz, *Antivir. Res.* **78**, 162 (2008).
- [4] G. Abramson and V. M. Kenkre, *Phys. Rev. E* **66**, 011912 (2002).
- [5] V. Kenkre, L. Giuggioli, G. Abramson, and G. Camelo-Neto, *Eur. Phys. J. B* **55**, 461 (2007).
- [6] J. A. Reinoso and F. J. de la Rubia, *Phys. Rev. E* **87**, 042706 (2013).
- [7] T. L. Yates, J. N. Mills, C. A. Parmenter, T. G. Ksiazek, R. R. Parmenter, J. R. Vande Castle, C. H. Calisher, S. T. Nichol, K. D. Abbot, J. C. Young *et al.*, *Bioscience* **52**, 989 (2002).
- [8] B. Hjelle and G. E. Glass, *J. Infect. Dis.* **181**, 1569 (2000).
- [9] C. H. Calisher, K. D. Wagoner, B. R. Amman, J. J. Root, R. J. Douglass, A. J. Kuenzi, K. D. Abbott, C. Parmenter, T. L. Yates, T. G. Ksiazek *et al.*, *J. Wildl. Dis.* **43**, 1 (2007).
- [10] E. R. Kallio, A. Poikonen, A. Vaheri, O. Vapalahti, H. Henttonen, E. Koskela, and T. Mappes, *Proc. R. Soc. B* **273**, 2771 (2006).
- [11] G. Abramson, V. M. Kenkre, T. L. Yates, and R. R. Parmenter, *Bull. Math. Biol.* **65**, 519 (2003).
- [12] G. Camelo-Neto, A. T. C. Silva, L. Giuggioli, and V. M. Kenkre, *Bull. Math. Biol.* **70**, 179 (2008).
- [13] S. A. Gourley and Y. Kuang, *Proc. R. Soc. Lond. A* **459**, 1563 (2003).
- [14] M. Abramowitz and I. A. Stegun, *Handbook of Mathematical Functions* (Dover, New York, 1970).
- [15] R. Fisher, *Ann. Eugenics* **7**, 355 (1937).
- [16] J. Murray, *Mathematical Biology*, 2nd ed. (Springer, New York, 1993).
- [17] F. M. Jaksic and M. Lima, *Austral Ecol.* **28**, 237 (2003).
- [18] Report on a “ratada” occurring in 2011 in western Argentina, <https://sites.google.com/site/rodentmanagement/feature-articles/reportonarataadaoccurringin2011inwesternargentina>